GENERALISED STACKING FAULT ENERGIES OF COPPER ALLOYS – DENSITY FUNCTIONAL THEORY CALCULATIONS

M. Muzyk [a*] and K.J. Kurzydlowski [b]

[a*] Faculty of Mathematics and Natural Sciences. School of Exact Sciences, Cardinal Stefan Wyszynski
University in Warsaw, Warsaw, Poland
[b] Faculty of Mechanical Engineering, Bialystok University of Technology, Białystok, Poland

Abstract

Generalised stacking fault energies of copper alloys have been calculated using density functional theory. Stacking fault energy of copper alloys is correlated with the d–electrons number of transition metal alloying element. The tendency to twiningis also modified by the presence of alloying element in the deformation plane. The results suggest that Cu –transition metal alloys with such elements as Cr, Mo, W, Mn, Re are expected to exhibit great work hardening rate due to the tendency to emission of the partial dislocations.

Keywords: Ab initio calculations; Copper alloys; Twining

1. Introduction

Copper and Cu based alloys are widely investigated due to high strength and high electrical and thermal conductivity [1–9]. High strength of copper alloys might be caused by nanoscale precipitates [10], deformation twining [11,12], and/or solid solutions strengthening [13]. Recently,an effort has been made to measure the influence of deformation twins on the mechanical behaviour of Cu [14] and Cu–based alloys: i.e. Cu–Al [15–17], Cu–Ag [1,18], Cu–Cr [19,20], Cu–Nb [7], Cu–Ta [21], Cu–Zn [22], Cu–Zr [23]. The evolution of nanotwinned copper leads to the high strength of materials [11,14].

Tadmor and Bernstein have shown that the tendency to deformation twining in a face–centered cubic (fcc) lattice depends on unstable stacking fault energy (USFE), and unstable twining energy (UTE) [24]. The unstable stacking fault energy is the maximum energy per unit area reached when one part of the crystal is shifted on a (111) plane along a [112] direction and the stacking fault is created. The unstable twinning energy is the maximum energy per unit area reached when one part of the crystal over stacking fault is shifted on a (111) plane along a [112] direction and the twin is created. However, the experimental measurement of these two values is impossible; USFE and UTE are determined by atomistic scale calculations [25,26]. These energies can be modified by the addition of appropriate alloying elements. The practical realization of Tadmor's and Bernstein's idea requires the estimation of the generalized stacking fault energy (GSFE) for the alloy. Such estimates can be currently obtained using computational methods. GSFEs have been computed for a number of fcc metals and their alloys, including Ni [27], Cu [21], Ti [28–30] and Al [25,31].

The latest theoretical works present GSFE calculation of Cu alloys [21,32]. Most recently Shao et al. have calculated GSFE of 18 substitutional atoms and 5 interstitial atoms with stacking fault (SF) in Cu [33]. It has been found that Sn, Al, Zn, P, Si and Ge can significantly decrease staking fault energy (SFE) of Cu solid solutions. Bhatia et al. have shown that GSFE calculations are crucial to understanding the experimental results in Cu–Ta alloys [21].

Experimental works concentrate on other Cu alloys, i.e. Cu–Zn [34], Cu–Be [35], Cu–Ni [36], Cu–Mg [37], but the GSFE calculations have not been carried out yet for the alloys. Thus, in the present study, density functional theory calculations have been used to analyse the effect of alloying elements on GSFE of copper alloys. The systematic calculations of GSFE of Cu and their alloys have been performed. Thirty elements in a substitutional position have been analyzed.

2. Calculations

Supercell contains twelve (111) planes with 2x2 slab geometry which gives 48 atoms in a system. The calculation of GSFE was performed by displacing one part of the crystal on the other along the ‹112› direction on a (111) plane in two operations: (i) one–half of the crystal was displaced,the maximum energy during the slip of the crystal is the USFE and the minimum is the SFE in Fig. 1;(ii) the second part of the crystal was displaced in the opposite direction (8–12 layers of a supercell) (see Figure 1 in Ref. [25]). The second maximum on the curves presented in Fig. 1 are the USFE and the following minimum is the TE. The alloying element was located in the place of Al atom in the slip plane. Taking into account the size of a supercell, the concentration of alloying elements was about 2at.% Vacuum space (6Å) and the relaxation of atom positions in perpendicular direction to free surface was applied. Cell shape and volume were kept fixed during the relaxation.

Vienna Ab–initio Simulation Package (VASP) [38,39] was used for density functional theory (DFT). Projector augmented wave potentials and generalised gradient approximation, with electron exchange–
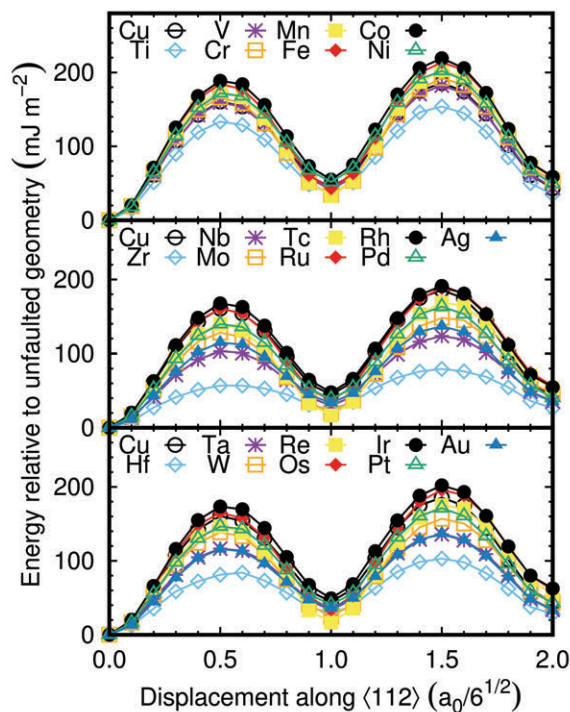
correlation described by Perdew–Burke–Ernzerhof (PBE) parameterization [40–43] were adopted for the GSFE calculations. Plane–wave cut–off energy of 400 eV, Fermi smearing of the electronic occupancy with 0.2 eV and 8x8x1 k–points mesh were used. The energy convergence greater than 10^{-4}eV for ionic relaxation was set.

3. Results

The Cu–GSFE calculation results are presented in Table 1.

Table 1. *The calculated values of unstable stacking fault energy (USFE), stacking fault energy (SFE),unstable twining energy (UTE) and twining energy (TE) for Cu. Available experimental (Exp.) and other calculations (Calc.) results are presented. All energies are in mJ/m²*

	USFE	SFE	UTE	TE	SFE/USFE	USFE/UTE
	161	45	186	42	0.280	0.865
Calc.	164[44], 158[45], 175[46], 181[47], 184[32]	38[44], 39[45], 41[47], 43[46], 47[32], 58[33]	168[48], 200[47], 217[32]	20[48], 53[32]		0.901[21]
Exp.	———	45[49] 40–45[50]	———	20–40[51]	———	———

Available experimental and other calculated data are included for comparison. The calculated values of GSFE's arein good agreement withother calculations and experimental data. It should be noted that TE is lower than SFE. The SFE/USFE is low in comparison to Al (0.862 [31]) and Mg (0.390 [26]), which means that partial dislocation emission (PDE) is easier in Cu of these three metals. The USFE/UTE ratio is close to the one from the metals (i.e. 0.791 in Al [31] and 0.827 in Mg [26]), which means that the twinnablity (TWA) of Cu is more favourable than Al and Mg.GSFE curves for Cu and selected alloys are presented in Fig. 1.

The results are described as follows: Cu – 3d, 4d, 5d transition metal (TM) alloys are described in sections 3.1, 3.2, 3.3, respectively; in section 3.4 Cu alloys with simple and post–TMs are described; the observed trends in GSFE values are described in section 3.5.

3.1 Stacking fault energies in copper in 3d transition metal alloys

Ti: In Cu–Ti alloys, up to 4wt.% Ti, yield strength and hardness increase linearly, due to solid–solution

Figure 1. *The generalised stacking fault energy (GSFE) of Cu and Cu–transition metal alloys. 3d, 4d and 5d elements are presented from top to bottom. The first and the second maxima are unstable stacking fault energy (USFE) and unstable twining energy (UT), respectively. The first and second minima are stacking fault (SF) and twining energy (TE) of the crystal in question*

Table 2. *Calculated values of unstable stacking fault energy (USFE), stacking fault energy (SFE), unstable twining energy (UTE) and twining energy (TE) for Cu and Cu–transition metal alloys. Available experimental and other calculations results are presented. All energies are in mJ/m²*

(3d)	Ti	V	Cr	Mn	Fe	Co	Ni	Cu
USFE	133	159	166	174	184	189	172 217[32] 269[52]	161
SFE	35 19*[53]	41	34	33 39*[54]	43	55	52 74[32]	45
UTE	154	182	192	203	214	219	202 180[32]	186
TE	35	44	53	57	58	59	49 77[32]	42
SFE/USFE	0.259	0.260	0.206	0.188	0.233	0.291	0.302	0.280
USFE/UTE	0.867	0.874	0.863	0.861	0.861	0.861	0.850	0.865
(4d)	Zr	Nb	Mo	Tc	Ru	Rh	Pd	Ag
USFE	57	103	128	140	160	168	140	115
SFE	24	29	20	16	37	48	39 80*[55]	34
UTE	80	124	148	169	188	191	163	137
TE	26	35	46	53	57	55	40	35
SFE/USFE	0.429	0.286	0.157	0.118	0.232	0.285	0.280	0.294
USFE/UTE	0.716	0.834	0.866	0.827	0.851	0.876	0.855	0.839
(5d)	Hf	Ta	W	Re	Os	Ir	Pt	Au
USFE	84	117	139	147	165	173	146	116
SFE	29	33	24	17	34	49	41	36
UTE	103	136	157	175	196	202	171	137
TE	28	34	44	55	60	63	43	33
SFE/USFE	0.350	0.284	0.176	0.113	0.207	0.284	0.277	0.313
USFE/UTE	0.817	0.858 0.847[21]	0.883	0.837	0.843	0.859	0.856	0.846

*Experimental data

hardening. In solution treated alloys marked changes are observed in hardness, strength, and elongation at about 4wt.% Ti, beyond which strength increases sharply and elongation decreases further, with increasing Ti content. This is attributed to fine scale precipitation of coherent Cu_4Ti phase [56,57]. Surface mechanical attrition treatment (SMAT) method employed to Cu–Ti alloys reveals that the density of mechanical twins first increases, and then decreases with a decrease in depth from the treated surface, and twining appears atlow strain and strain rate region [53]. The deformation mechanism changes from twining to dislocation activities with increasing strain and strain rate. SFE/USFE is lowered by Ti, so the partial dislocations emission is enhanced. USFE/UTE is almost unchanged in relation to Cu, TWA is unchanged as well. Mechanism of twins formation in SMATed Cu–4wt.%Ti can have an origin in mechanical alloying (MA) method, where high strains are applied. The SFE and TE have the same value (35 mJ/m²), which is one of the lowest ones in 3d TMs. Due to high energy and high strain method of synthesis, the criterion adopted in our calculations to twin nucleation analyse (USFE/UTE) may by beyond applicability in SMATed Cu–Ti alloys. However, low value of SFE and TE facilitate the formation of planar defects as is observed in Cu–Ti alloys.

V: Cu–V alloys are not widely investigated. Twins

and stacking faults (SFs) have not been found in Cu/V multilayers structures fabricated by cross accumulative roll bonding method [58], but SFs have been observed in coherent Cu/V layers as a response to the strain due to atom size misfit between Cu and V [59]. The Cu/V layers were sputter–deposited onto [001] Si substrates. The GSFE and related values are almost unchanged in Cu–V solid solution. Nosignificant effect to mechanical properties due to vanadium amountis expected.

Cr: The class of Cu–Cr alloys are well known types of precipitation–hardened copper based alloys.Through annealing and quenching, the size of the precipitations from about10 nm [19] up to 500 nm [60] have been found. Moreover, precipitation strengthened Cu–Cr alloy processed by equal–channel angular pressing (ECAP) has high strength, high conductivity and sufficient ductility. The grain refinement combined with alloying is an optimal approach to enhance the tensile property and fatigue performance of materials [61,62]. The presence of Cr precipitations reduces the mobility of dislocations and boundaries, and hinders them to slip, which leads to much more stable and denser dislocations distribution clustering near the boundaries and precipitations [13]. Annealing and quenching lead to form the supersaturated solid solution [60]. Severe plastic deformation (SPD) procedure also leads to dissolution of Cr precipitates [63]. Guo et al. have shown that after high pressure torsion (HPT) treatment of Cu–43wt.% Cr two phase alloy about 30.5wt.% (26.4at.%) of Cu atoms has been dissolved into Cr grains, simultaneously Cu grains contain about 3.9wt.% (4.7at.%) Cr dissolved inside [64]. GSFE calculation showed that PDEis improved by Cr atoms into Cu matrix; TWA is almost unchanged. Experimental results referee high strength and ductility of Co–Cr alloys, as a results of grain refinement, cold deformation and precipitation strengthening mechanisms [13,19,61]. The effect of Cr on GSFE vs. to grain refinement after eight ECAP process looks negligible [63].

Mn: Slightly different deformation modes in Cu–Al and Cu–Mn suggest different values of SFE in both alloys [65]. Wu et al. suggested that twin density does not play a major role in promoting the strain hardening (less than 0.1%) and manganese addition has a minor effect on SFE value of Cu–Mn alloys [66]. However, they have found that structural investigation of NC Cu–Mn alloys with different Mn contents reveals that the Mn content causes increasing dislocation density [66]. Indeed, the USFE/UTE value of Cu–Mn alloys does not give the promotion of twin formation but the low value of SFE/USFE suggests that partial dislocation slip may occur andductility is enhanced bypartial dislocations emission. Engler found that with increasing Mn contents transition from the copper– to the brass–type texture was observed ($\{1\overline{1}2\}\langle111\rangle$to$\{011\}\langle211\rangle$). The rolling textures of Cu–Mn alloys strongly resembled the results obtained in rolling Cu–Zn system as a result of decreasing SFE [67] and Engler explained that with short–range ordering. The SFE and the SFE/USFE indicate that effect of Mn to GSFE may be underestimated and partial dislocations may play an important role on ductility enhanced.

Fe: MA of Cu–Fe powder or SPD treatment of two phase alloy leads to the formation of supersaturated fcc solid solutions with up to 60–70 at.% Fe in Cu [68–71], whereas equilibrium state has shown immiscibility between Cu and Fe [6]. Fu et al. have found that by powder metallurgy (combustion synthesis) nanostructured matrix with dendrite composite Cu–Fe alloy can be successfully obtained [72]. Dendrite and matrix are Fe(Cu) solid solution (34.41at.% Cu) and Cu(Fe) solid solution (19.95at.% Fe), respectively. The yield strength, the ultimate strength and the plastic strain in compression test of the alloy are 540 MPa (which is higher than that of commercial crystalline Cu–Fe), 1050MPa and 20.9%, respectively. Nanostrucutured composite $Cu_{60}Fe_{40}$ alloy exhibits high strength and enhanced ductility due to remarkable work hardening. Zhang et al. have found that the TA of Cu–Fe alloys is almost independent of Fe concentrations [73]. GSFE calculations reveal that PDEis significantly improved in Cu–Fe alloy, whereas TA remains unchanged vs. Cu. High work hardening rate exhibits that Fe effect in Cu may be similar to Mn effect in Cu matrix.

Co: Both the as–deformed and annealed Cu–26at.% Co alloy samples combined high tensile strength withgood ductility andductile fracture behaviour [74], which is achieved by nanoscale composite structure as a result of annealing supersatured solid solution. SFE/USFE ratio is higher than in Cu, which means that PDEis impede. Cu–Co alloy have enhanced mechanical properties, but the effect of Co on GSFE looks negligible.

Ni: The Cu–Ni alloys exhibit increased tensile strength together with the maintenance of high ductility with increasing Ni content, whereas SFE increases with increasing Ni content [55,75,76]. Wang et al. [54] have shown that with increasing Ni content from 5 to 20at.%, the yield strength and ultimate tensile strength of Cu–Ni alloys keep increasing at nearly no expense of uniform elongation; planar–slip bands were observed indicating that short–range ordered structures such as short–range clusters in Cu–Ni alloys are beneficial to the promotion of planar slip in such a high SFE crystal lattice. Indeed the SFE, USFE, UTE and TE values increase in Cu–Ni alloy and deformation by full dislocation emission is promoted, even the Ni–Cu do not shear at all in cube–on–cube interface test [77]. The enhanced activity of

cross slip due to influencing factors such as high SFE value leads to a specific dislocation microstructure with increasing Ni content, in order, dislocation cells, cell block structure and extended dislocation walls [54].

3.2 Stacking fault energies in copper in 4d transition metal alloys

Zr: Cu–Zr alloys are a class of the bulk metallic glasses materials, which have been intensivelyinvestigated recently [78–80]. However, in crystal state the Cu–Zr alloys are investigated as well. Kauffmann et al. have investigated the influence of Zr addition in the form of solute atoms as well as nano–size Cu_5Zr precipitates on the recrystallization of cryo–drawn Cu. It has been found that deformation twining was active during deformation in liquid nitrogen in Cu–(0.7,0.14 and 0.21) at.% Zr alloys and leads to increasing dislocation density, deformation twining and a refinement of the microstructure [4]. In Cu/Cu–Zr nanolaminated structure neither heavy dislocation storage nor increased SFs and deformation nanotwins were observed in Cu nanolayers, indicating that nucleated dislocations can be absorbed by Cu/Cu–Zr interfaces [81]. Li et al. have found the deformation twins and shear bands withinlamellar structure of the cryogenically rolled Cu–Zr alloy contribute to grain refinement and improve mechanical properties [23].GSFE calculation shows that SFE/USFE ratio is extremely high in Cu–Zr alloy in comparison to other analysed Cu alloys, but SFE and TE are very low. The stability of these defects is high andtwins are observed. The case of Cu–Zr alloy shows that SFE/USFE criterion is not a general one. In the case of Cu–Zr alloys the atom size mismatch may play a significant role as well.

Nb: Addition of 1at.% Nb to Cu greatly affects its mechanical properties and deformation mechanism. The ultra–high yield and ultimate tensile strengthsare achieved simultaneously with good ductility and strain hardening of the NC Cu–1at.% Nb than that of the NC Cu have been observed [7]. These improved properties are the effect of smaller grain size (it has been found that Nb atoms stabilize effectively grain size in Cu [82,83]), solid solution hardening, andlattice stresses associated with supersaturation of Nb in Cu matrix.GSFE shows thatall energies decrease then in Cu and SFE/USFE is lowered by Nb as well. Partial dislocation may be emitted more easily due to Nb content in Cu matrix.

Mo: SFE, SFE/USFE and USFE/UTE values indicate that twining and PDEare facilitated by Mo addition. Mo addition to Cu causes grain sizes and SFE decrease and strain, dislocation density, SF probability, and hardness increase of Cu–Mo alloys [84]. Cornejo et al. have found that during the MA

process Cu–Mo alloys exhibit up to 2.4wt.% Mo solubility in Cu matrix [85].

Tc: Technetium significantly facilitate PDE due to low SFE/USFE value. TWA is decreased due to high twin energy.

Ru: In immiscible Cu–Ru alloyssolid solution has been successfully formed [86,87]. No mechanical test of the Cu–Ru alloys has been performed yet. Decreasing of SFE and SFE/USFE and increasing USFE/UTE ratio indicate that TA should be improved.

Rh: Rhodium atoms may form solid solution in Cu up to 20at.% Rh in low temperatures and the element possesses unlimited solubility in Cu at high temperatures [88].GSFE is almost unchanged in Cu–Rh alloy in comparison to Cu. The TWA (USFE/UTE) is slightly increased.

Pd: SFE varies non linearly with the composition due to the ordering ofstructure [55]. Lu et al. have calculated the SFE vs. Pd concentration showing that the element increases the SFE [75]. Our GSFE calculation shows that Pd atom decreases GSFE, but does not change SFE/USFE parameter and slightly decreases USFE/UTE. The TA of Cu is not improved by Pd addition.

Ag: The addition of Ag facilitates the introduction of nanoscale deformation twins in solid solution samples; this nanosized twins, grains, and precipitates imparthigh strength ofmaterials based ongrain refinement andprecipitation strengthening [1,89]. The Cu–28wt.% Ag alloy displays a much stronger strain hardening rate than Cu [18] andmechanical properties of alloys are effectively improved by SPD method [90–92] and heat treatment [2,3,93]. Deformation by twins is widely observed in Cu–Ag alloys [1,89,90]. Our results have shown thatUSFE, SFE, UTE and TE are decreased by Ag. However,SFE/USFE indicates thatPDEand twins formation should be weakened. In Cu–Ag alloyshardening is caused not only by the effect of lowering SFE, but precipitation hardening plays an important role as well [93].

3.3 Stacking fault energies in copper in 5d transition metal alloys

Hf: Hf atom decreases the values of USFE, SFE, UTE and TE, but increases SFE/USFE ratio and impedespartial dislocation emission.USFE/UTE ratio indicates that TA decreases. Mechanical testing of Cu–Hf system has not been found. Cu–Hf solid solution does not promise enhanced mechanical properties.Phase stability experiment gives enthalpy of mixing about –150 meV/atom and alloys tends to form ordered structures [94,95].

Ta: Bhatia et al. [21] have used semi–empirical embedded atom potential (EAM) developed by Pun et al. [96]. They have found that Ta causes the decrease of USFE and the increase of SFE and UTE. DFT

Table 3. *Calculated values of unstable stacking fault energy (USFE), stacking fault energy (SFE), and unstable twining energy (UTE) for Cu and Cu alloys. Available experimental and other calculations results are presented. All energies are in mJ/m²*

	Cu	Mg	Al	Si	Zn	Ga	Ge	Sn
USFE	161	117	135	137	140	119	116	72
			165[32]		161[32]	156[32]		
			169[47]					
SFE	45	19	7	10	19	5	7	–7,
			7[47],	3[109],	18[112],	~1*[115],	8–15[118],	3–4[119]
			8[32],	10*[110],	21[32],	3[32],	62[33],	6–42[120]
			7*[106],	5–25*[108],	35[22],	~9[116],	3–35*[108]	39[108]
			12–61[107],	3*[111]	*14–35*[113,114],	2–30*[108],		76[33],
			4–37[108]		*12–35*[108]	10*[117],		11–33*[108]
UTE	186	132	134	133	146	118	113	69
			176[47],		178[32]	161[32]		
			180[32]					
TE	43	20	3	–5	13	1	–7	–14
			17[32],		25[32]	1[32]		
SFE/USFE	0.278	0.160	0.055	0.073	0.134	0.040	0.057	–0.095
USFE/UTE	0.865	0.889	1.002	1.024	0.959	1.013	1.019	1.041
T	1.018	1.048	1.129	1.138	1.093	1.137	1.138	1.169
			1.11[47]					

*Experimental data

calculations have shown that Ta significantly decreases USFE, SFE and UTE, which is a general trend in TMs with decreasing d electrons (see Table 2). The mechanical properties of mechanically alloyed Cu–Ta composites are dependent on the microstructural evolution [97]. The coherent particles promotetwining deformation, whereas the incoherent ones – dislocations [21].

W: Recent progress in Cu–W synthesis and mechanical testing has found satisfactory mechanical properties [98–102]. The Cu–W alloys are usually obtained by MA due to huge difference in melting point between elements. Characterisation is mainly focused ondensity, Cu/W cohesion and hardness [99], showing good mechanical properties and composite–like structure [101]. GSFE prompts that tungsten atom in Cu matrix leads to improved properties, i.e. ductility. SF and twins have not been observed yet in Cu–W alloys, but there ishigh probability that deformations may be realized by partial dislocation. This is because SFE/USFE ratio is greatly decreased by W.

Re: In metals with 5d electrons shell Re is the most promising element to enhance Cu properties. This is due to the lowest SFE/USFE ratio. PDEis greatly improved. Cu–Re alloy has not been mechanically tested yet. GSFE curve suggests that Re enhances mechanical properties of Cu even in small amount.

Os: Osmium atom in Cu matrix leads to the decrease of SFE, SFE/USFE and the increase of USFE, UTE and TE. PDEis facilitated by impurity, but TWA is not changed. Mechanical testing of Cu–Os alloys is not available, but GSFE calculation reveals that strain hardening rate may be improved bythe alloying element.

Ir: GSFE of Cu–Ir alloy indicates that the tendency of partial dislocations emission and twins formation is decreased. There is no mechanical testing of Cu–Ir system, but ab initio prediction suggests that the properties are not improved by Ir atoms in Cu matrix.

Pt: Recent calculation using the exact muffin–tin orbitals (EMTO) method in combination with coherent potential approximation (CPA) reveals that SFE increase is almost linear with Pt concentration [75]. GSFE curve shows thatUSFE, SFE and UTE are slightly lowered by Pt. The absence of mechanical testing of Cu–Pt impedes discussion about the Pt effect. Experimental investigation of ordered Cu–Pt alloys have shown that twin formation can occur in$\{111\}\langle11\bar{2}\rangle$ slip system [103], butalloys preferfull dislocation emission as is generally in ordered

structures [49].

Au: Cu–Al alloys form ordered structures [104]. Volkov has found high strength and ductility of ordered Cu–Au alloys, the highest mechanical properties of an equiatomic Cu–Au alloy can be obtained if its structure is refined as much as possible. The retardation of recrystallization and quick ordering provide the best result [105]. GSFE calculation predicts that in fcc–Cu–Al alloy SFE and TE is lowered by the alloying element. The highest SFE/USFE and USFE/UTE values than in Cu suggest thatPDEand twining are impeded. The formation energy of equiatomic composition of ordered Cu–Au is about –90 meV/atom [104]. The structure consists of alternate planes of Cu and Au atoms perpendicular toc–axis and leads to tetragonal cell as a consequence of different atomic size. The model used in present calculation does not take into account the ordering effect. GSFE calculations of ordered Cu–Al alloys are needed to understand the alloys' mechanical properties.

3.4 Stacking fault energy of Cu – non transition metals alloys

Mg: High twins density has been found in Cu–Mg alloy after the high deformation and recrystallization process [37].The enhanced strength and ductility in the alloy have been achieved. Many twins were observed from the microstructure of the Cu–0.4wt.%Mg alloy, and only a few twins were observed on the Cu–0.2wt.% Mg alloy. This indicates that Cu may be very sensitive to Mg concentration. Moreover, the effectiveness of work hardening was improved due to Mg concentrations [5]. SFE/USFE and USFE/UTE values show thattwining is promoted by Mg atoms in Cu matrix.

Al: Aluminium leads to high reduction of SFE in Cu alloy. The enhanced strength and ductility are widely observed in Cu–Al alloys [15,121–124]. Decreasing the SFE in Cu and Cu–Al alloys leads to lower twins spacing from 11.7 nm to 2.0 nm in Cu and Cu–6wt.% Al, respectively [123]. Low SFE and TE improve the strength–ductility synergy as well [125]. The remarkable effect of SFE on the grain refinement of Cu–Al alloys was attributed to the transition of dominant deformation mechanism from subgrain subdivision by in–grain dislocation activity to deformation twining and shears banding. The critical value of SFE for this transition was found at SFE 28 mJ/m^2 corresponding to an Al content of about 5at.% in Cu [126]. Aluminium addition changes SFE/USFE and USFE/UTE more than Mg atom. The mechanical properties are improved significantly, which is confirmed by the experimental results.

Si: Barret has found that thermal treatment of Cu–Si alloys introduces high density of SFs. The distance between them is five to ten atomic layers [127]. The observed texture of Cu–Si alloy after cold–rolling and recrystallization corresponds to twining process [111]. Suzuki segregation of Si atoms to SFs has been observed as well [128,129], which suggests that Si decreases SFE. The calculated GSFE values of Cu–Si show that TWA of the alloy is very high and may be compared to Cu–Al alloys. The negative value of TE means that the structure of Cu–Si is unstable, and phase transformation occurs with increasing Si content [130]. Recently,the mechanical properties of Fe–Cu alloys are enhanced by Si, which facilitates the precipitation hardening [131].

Zn: The SFE of Cu–Zn decreases with the increasing Zn concentration [108,113]. Average grain sizes and the width of twins decreasing, and the density of twins increasing with decreasing SFE in HPT processing Cu–Zn alloys were found [114]. Xiao et al. have found that the mechanical twining in Cu–32wt.% Zn commercial brass is realized by continuous creations of new twins between the pre–existing TB spacing until the TB spacing is close to 10 nm [132]. GSFE calculation reveals lower SFE in Cu–Zn alloys than in pure Cu. Low SFE of the nanocrystaline Cu–Zn–Al alloys greatly affect its mechanical properties and deformation mechanism as well. Yield strength is increased about 35% in Cu–Zn–Al alloys than of Cu [133]. GSFE results confirm the well-known in the case of Cu–Zn mechanical properties. Low values of SFE/USFE and USFE/UTE close to 1.0 indicate that PDE and twining are the most promoted deformation mechanisms.

Ga: Experimental results indicate that dislocations, SFs and twins density increase with increasing Ga concentration [115]. SFE tends to zero with increasing Ga concentration [134]. Low SFE, SFE/USFE should improve ductility of the Cu alloy. There are no available results of mechanical testing of Cu–Ga alloy. The alloy may have mechanical properties similar to Cu–Ge, Cu–Al and Cu–Si.

Ge: The reduction of SFE, very low value of SFE/USFE, and USFE/UTE close to 1.0 indicate high strength and high ductility of Cu–Ge alloy. Experimental results confirm that the alloy tends to increase in dislocation density and twin density, which contributes to the improvements in the mechanical properties by strain hardening rate; high strength, and excellent ductility can be simultaneously achieved in Cu–Ge alloy [135]. Reducing SFE can be an effective approach to produce the alloys with optimal mechanical properties [118].

Sn: A lot of effort has been made on TWA of Cu–Sn and Cu–Sn–based alloys [112,119,120,136–138]. The negative value of SFE and TE in fcc Cu–Sn is the effect of the observed phase transition to D0$_{19}$ ordered structure in high Cu concentration alloys [137,138]. GSFE of Cu–Sn calculated in fcc lattice show a

significant decreasein energies. Bronze is a ductile alloy, and GSFE in ordered structure may give us important information about the deformation mechanism on atomic scale level [139].

High SFE confines separation of partial dislocations, which facilitates cross–slip. As such, dislocations show irregular wavy shapes and easily tangle together to form three–dimensional dislocation cells. Low SFE leads to the formation of extended partial dislocations which are difficult to cross–slip. Therefore, large amounts of planar arrays dominate plastic deformation of the low SFE materials [140].

3.5 Trends in the energies in Cu alloys

Figures 2 a)–c) show the trends in SFE, USFE and UTE in Cu–TMs alloys in function of valence electrons (VEs) in alloying element. SFE has a lower value for 7 VEs metals in all periods. USFE and UTE decrease up to 9 VEs, then energies go down. SFEs in 4d and 5d have very similar values as well as USFE and UTE ones. Only four elements increase SFE: Co, Rh, Ir and Ni (the points are above the line, which indicates the SFE for Cu on Fig. 2). SFE is lowered by
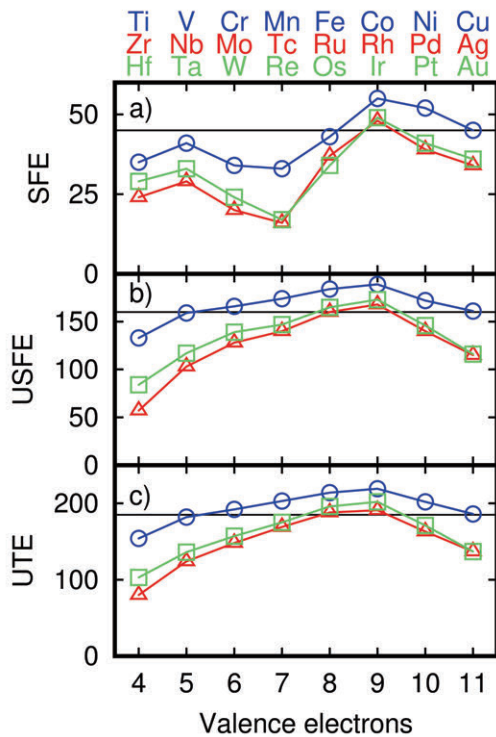
other analysed metals as well (see Table 3). Especially, Al, Si, Ga and Ge reduce SFE. USFE and UTE are significantly increased by 3d metals. The highest values of these energies have the 9 VEs elements. There are the same elements which have the highest values of SFE (Co, Rh, Ir).

SFE/USFE in Cu – TMs alloys are plotted on Fig. 3. The lowest SFE/USFE value means PDE is facilitated due to the effect of alloying element. The analysed value has a specific shape. Zr and Hf increase the value significantly and impede PDE. The lowest value is for metals with 7 valence electrons (VEs). However, elements with 6 and 8 VEs exhibit promising values as well. SFE/USFE for 9–11 VEs elements are very close to Cu value (0.280) and do not change PDE tendency. Rhenium is the most promising element from the point of view of PDE tendency. USFE/UTE ratio is plotted on Fig. 4. As we can see, there is no significant change in values, except for Zr and Hf. Increasing USFE/UTE increases TWA. The results do not show a significant trend in the TWA as in the case of PDE (Fig. 3).

In four Cu– alloys: –Al, –Mo, –Ti, and –Zr, twin friction has been compared [84]. The experimental results show that twin friction increases in these alloys as follows: Al>Ti>Mo>Zr, which is exactly confirmed by increasing SFE/USFE value in our calculations. Based on GSFE calculations and available experimental data of the mechanical properties of Cu alloys discussed in sections 3.1–3.3 we can see that in many cases (i.e. Ti, Nb, Ta, Mn) PDE and twins are observed, whereas USFE/UTE value does not predict

Figure 2. *The trends in energies: a) stacking fault energy (SFE), b) unstable stacking fault energy (USFE), c) unstable twining energy (UTE) in Cu– transition metals alloys in function of valence electrons (VEs) in alloying element. Black tiny lines are the analysed value for Cu. SFE has a lower value for 7 VEs metals in all periods. USFE and UTE decrease up to 9 VEs, then energies go down. The energies are in mJ/m²*

Figure 3. *The stacking fault energy (SFE) to unstable stacking fault energy (USFE) ratio in Cu – transition metals alloys. The thiny black line shows the SFE/USFE value for Cu (0. 280). The lowest SFE/USFE value means the partial discloation emision (PDE) increases due to the effect of the alloying element. The analysed value has a specific shape. Zr and Hf increase the value significantly and impede the PDE. The lowest value is for metals with 7 valence electrons (VEs), which are the most promising transion metals elements from PDE point of view. With increasing VEs the SFE/USFE increases to the value of Cu*

TWA enhanced. SFE and SFE/USFE values of these alloys have lower values than Cu. Thus in Cu alloys the USFE/UTE criterion may be irrelevant in the case of TWA predictions.

Zhang et al. present the GSFE calculation on 42 Cu alloys [73]. They have found that for 16 Cu–TMs alloys the USFE and SFE is 164 and 53–54 mJ/m^2,respectively, which means that the elements do not have an impact on deformation mechanism; our results show that the impact is crucial. Moreover, i.e. the SFE in Cu–1at.% Si is below zero, which suggests that the fcc structure is unstable, but the Cu–Si phase diagram shows that up to ~8at.% Si the fcc structure is stable [73].
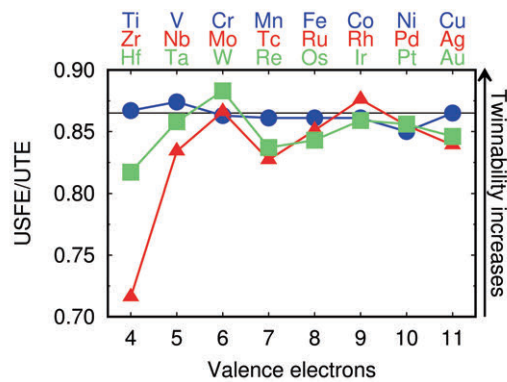
Figure 4. *The unstable stacking fault energy (USFE) to unstable twining energy (UTE) ratio is the measure of the twinnability. Increasing USFE/UTE increases the twinnability. The tiny black line is the USFE/UTE value for Cu (0.865). The results do not show a significant trend in the twinnability as in the case of the PDE(Fig. 4). Except Zr, the values are close to the 0.865*

4. Conclusion

Thirty Cu alloys have been analysed from the point of view of PDE and TWA. GSFE results have been confirmed by observed SF and twins in Cu alloys.

(1) The computational and experimental results show that TMs with 6–7 VEs are the most promising from the point of view ofenhanced strength and ductility of Cu alloys (Cr, Mo, W, Mn, Re).

(2) The all non–transition analysed elements enhanced PDE and TWA.

(3) Specific trends have been observed in SFE, USFE, and UTE as well as in SFE/USFE and USFE/UTE as a function of valence electrons number in alloying element.

(4) The experimental observations of SF and twins formation in Cu alloys confirm our GSFE predictions.

(5) Deformation mechanism of Cu alloys can be governed effectively by TMs elements. The results identify the most promising Cu alloys from the enhanced mechanical properties point of view.

References

[1] B.B. Zhang, N.R. Tao, K. Lu, Scr. Mater., 129 (2017) 39–43.

[2] Y. Sakai, H.J. Schneider-Muntau, Acta Mater., 45 (1997) 1017–1023.

[3] Y. Sakai, T. Hibaru, K. Miura, A. Matsuo, K. Kawaguchi, K. Kindo, MRS Adv., 1(2016) 1137–1148.

[4] A. Kauffmann, D. Geissler, J. Freudenberger, Mater. Sci. Eng. A, 651 (2016) 567–573.

[5] C. Zhu, A. Ma, J. Jiang, X. Li, D. Song, D. Yang, Y. Yuan, J. Chen, J. Alloys Compd., 582 (2014) 135–140.

[6] S.F. Abbas, S. Seo, K.-T. Park, B. Kim, T. Kim, J. Alloys Compd., 720 (2017) 8–16.

[7] K.M. Youssef, M.A. Abaza, R.O. Scattergood, C.C. Koch, Mater. Sci. Eng. A ,711 (2018) 350–355.

[8] J. Han, J. Sun, Y. Han, H. Zhu, L. Fang, Metals (Basel)., 8 (2018) 344.

[9] A. Hosseinzadeh Delandar, R. Sandström, P. Korzhavyi, Metals (Basel)., 8 (2018) 772.

[10] Q. Lei, Z. Li, M.P. Wang, L. Zhang, Z. Xiao, Y.L. Jia, Mater. Sci. Eng. A, 527 (2010) 6728–6733.

[11] L. Lu, X. Chen, X. Huang, K. Lu, Science., 323 (2009) 607–610.

[12] J. Sun, C. Li, J. Han, X. Shao, X. Yang, H. Liu, D. Song, A. Ma, Metals (Basel)., 7 (2017) 438.

[13] C.Z. Xu, Q.J. Wang, M.S. Zheng, J.W. Zhu, J.D. Li, M.Q. Huang, Q.M. Jia, Z.Z. Du, Mater. Sci. Eng. A, 459 (2007) 303–308.

[14] L. Lu, Y. Shen, X. Chen, L. Qian, K. Lu, Science., 304 (2004) 422–426.

[15] Y. Zhang, N.R. Tao, K. Lu, Scr. Mater., (2009).

[16] H. Xu, I. Qin, H. Clauberg, B. Chylak, V.L. Acoff, Scr. Mater., 115 (2016) 1–5.

[17] C.W. Schmidt, P. Knödler, H.W. Höppel, M. Göken, Metals (Basel)., 1 (2011) 65–78.

[18] Y.Z. Tian, S.D. Wu, Z.F. Zhang, R.B. Figueiredo, N. Gao, T.G. Langdon, Scr. Mater., 65 (2011) 477–480.

[19] R.K. Islamgaliev, K.M. Nesterov, J. Bourgon, Y. Champion, R.Z. Valiev, J. Appl. Phys., 115 (2014) 1–5.

[20] X. Chen, F. Jiang, J. Jiang, P. Xu, M. Tong, Z. Tang, Metals (Basel)., 8 (2018) 227.

[21] M.A. Bhatia, M. Rajagopalan, K.A. Darling, M.A. Tschopp, K.N. Solanki, Mater. Res. Lett., 5 (2017) 48–54.

[22] L.I. Zaynullina, I. V Alexandrov, W. Wei, Defect Diffus. Forum, 385 (2018) 195–199.

[23] R. Li, S. Zhang, H. Kang, Z. Chen, F. Yang, W. Wang, C. Zou, T. Li, T. Wang, J. Alloys Compd., 693 (2017) 592–600.

[24] E.B. Tadmor, N. Bernstein, J. Mech. Phys. Solids, 52 (2004) 2507–2519.

[25] M. Muzyk, Z. Pakiela, K.J. Kurzydlowski, Scr. Mater., 64 (2011) 916–918.

[26] M. Muzyk, Z. Pakiela, K.J. Kurzydlowski, Scr. Mater., 66 (2012) 219–222.

[27] D.J. Siegel, Appl. Phys. Lett., 87 (2005) 121901–3.

[28] P. Kwasniak, M. Muzyk, H. Garbacz, K.J. Kurzydlowski, Mater. Chem. Phys., 154 (2015) 137–143.

[29] P. Kwasniak, M. Muzyk, H. Garbacz, K.J. Kurzydlowski, Mater. Lett., 94 (2013) 92–94.

[30] P. Kwasniak, M. Muzyk, H. Garbacz, K.J. Kurzydlowski, Mater. Sci. Eng. A, 590 (2014) 74–79.

[31] M. Muzyk, Z. Pakieła, K.J. Kurzydłowski, Metals (Basel)., 8 (2018) 823.

[32] W. Li, S. Lu, Q.-M.M. Hu, S.K. Kwon, B. Johansson, L. Vitos, J. Phys. Condens. Matter, 26 (2014) 265005.

[33] Q.Q. Shao, L.H. Liu, T.W. Fan, D.W. Yuan, J.H. Chen, J. Alloys Compd., 726 (2017) 601–607.

[34] G.H. Xiao, N.R. Tao, K. Lu, Scr. Mater., 65 (2011) 119–122.

[35] J.C. Pang, Q.Q. Duan, S.D. Wu, S.X. Li, Z.F. Zhang, Scr. Mater., 63 (2010) 1085–1088.

[36] A. Shadkam, Scr. Mater., 135 (2017) 68–71.

[37] L. Song, Y. Yuan, Z. Yin, Int. J. Nonferrous Metall., 2 (2013) 100–105.

[38] G. Kresse, J. Furthmüller, Comput. Mater. Sci., 6 (1996) 15–50.

[39] G. Kresse, J. Furthmüller, Phys. Rev. B - Condens. Matter Mater. Phys., 54 (1996) 11169–11186.

[40] P.E. Blöchl, Phys. Rev. B, 50 (1994) 17953–17979.

[41] J.P. Perdew, K. Burke, M. Ernzerhof, Phys. Rev. Lett., 77 (1996) 3865–3868.

[42] J.P. Perdew, K. Burke, M. Ernzerhof, Phys. Rev. Lett., 77 (1996) 3865–3868.

[43] D. Joubert, Phys. Rev. B - Condens. Matter Mater. Phys., 59 (1999) 1758–1775.

[44] C. Brandl, P.M. Derlet, H. Van Swygenhoven, Phys. Rev. B - Condens. Matter Mater. Phys., 76 (2007) 1–8.

[45] S. Ogata, J. Li, S. Yip, Science (80-.)., 298 (2002) 807–811.

[46] X.Z. Wu, R. Wang, S.F. Wang, Q.Y. Wei, Appl. Surf. Sci., 256 (2010) 6345–6349.

[47] S. Kibey, J.B. Liu, D.D. Johnson, H. Sehitoglu, Appl. Phys. Lett., 89 (2006) 191911.

[48] S. Ogata, J. Li, S. Yip, Phys. Rev. B, 71 (2005) 224102.

[49] J.P. Hirth, J. Lothe, Theory of Dislocations, 2nd ed., Wiley, New York, 1982.

[50] C.B. Carter, I.L.F. Ray, Philos. Mag., 35 (1977) 189–200.

[51] J.M. Howe, Interfaces in Materials, Wiley, New York, 1997.

[52] S. Shao, J. Wang, Metals (Basel)., 5 (2015) 1887–1901.

[53] H. Wei, Y. Cui, H. Cui, C. Zhou, L. Hou, Y. hui Wei, J. Alloys Compd., 763 (2018) 835–843.

[54] Z.Y. Wang, D. Han, X.W. Li, Mater. Sci. Eng. A, 679

(2017) 484–492.

[55] I.R. Harris, I.L. Dillamore, R.E. Smallman, B.E.P. Beeston, Philos. Mag., 14 (1966) 325–333.

[56] S. Nagarjuna, M. Srinivas, K. Balasubramanian, D.S. Sarma, Mater. Sci. Eng. A, 259 (1999) 34–42.

[57] J. Stasic, D. Bozic, J. Alloys Compd., 762 (2018) 231–236.

[58] S. Wei, L. Zhang, S. Zheng, X. Wang, J. Wang, Scr. Mater., 159 (2019) 104–108.

[59] Q. Guo, G.B. Thompson, Acta Mater., 148 (2018) 63–71.

[60] A. Korneva, B. Straumal, A. Kilmametov, R. Chulist, P. Straumal, P. Zieba, Mater. Charact., 114 (2016) 151–156.

[61] W. He, E. Wang, L. Hu, Y. Yu, H. Sun, J. Mater. Process. Technol., 208 (2008) 205–210.

[62] Q.J. Wang, Z.Z. Du, L. Luo, W. Wang, J. Alloys Compd. 526 (2012) 39–44.

[63] K.X. Wei, W. Wei, F. Wang, Q.B. Du, I. V Alexandrov, J. Hu, Mater. Sci. Eng. A 528 (2011) 1478–1484.

[64] J. Guo, J. Rosalie, R. Pippan, Z. Zhang, Scr. Mater. 133 (2017) 41–44.

[65] A. Nortmann, C. Schwink, Acta Mater., 45 (1997) 2051–2058.

[66] X.X. Wu, X.Y. San, X.G. Liang, Y.L. Gong, X.K. Zhu, Mater. Des., 47 (2013) 372–376.

[67] O. Engler, Acta Mater. 48 (2000) 4827–4840.

[68] J. Eckert, J.C. Holzer, C.E.K. Iii, W.L. Johnson, J. Appl. Phys., 73 (1993) 2794–2802.

[69] A. Bachmaier, M. Kerber, D. Setman, R. Pippan, Acta Mater., 60 (2012) 860–871.

[70] M. Mojtahedi, M. Goodarzi, M.R. Aboutalebi, M. Ghaffari, V. Soleimanian, J. Alloys Compd., 550 (2013) 380–388.

[71] N. Wanderka, U. Czubayko, V. Naundorf, V.A. Ivchenko, A.Y. Yermakov, M.A. Uimin, H. Wollenberger, Ultramicroscopy, 89 (2001) 189–194.

[72] L. Fu, J. Yang, Q. Bi, W. Liu, Philos. Mag. Lett., 91 (2011) 78–85.

[73] Y. Zhang, J. Guo, J. Chen, C. Wu, K.S. Kormout, P. Ghosh, Z. Zhang, J. Alloys Compd., (2018).

[74] A. Bachmaier, G.B. Rathmayr, J. Schmauch, N. Schell, A. Stark, N. Jonge, R. Pippan, J. Mater. Res., 1 (2018) 1–11.

[75] S. Lu, Q. Hu, E.K. Delczeg-Czirjak, B. Johansson, L. Vitos, Acta Mater., 60 (2012) 4506–4513.

[76] S. Koda, J. Phys. Soc. Japan, 19 (1964) 2356–2357.

[77] X. Liu, R. Hao, S. Mao, S.J. Dillon, Scr. Mater., 130 (2017) 178–181.

[78] S.W. Lee, M.Y. Huh, E. Fleury, J.C. Lee, Acta Mater., 54 (2006) 349–355.

[79] N. Mattern, P. Jóvári, I. Kaban, S. Gruner, A. Elsner, V. Kokotin, H. Franz, B. Beuneu, J. Eckert, J. Alloys Compd., 485 (2009) 163–169.

[80] D. Wang, Y. Li, B.B. Sun, M.L. Sui, K. Lu, E. Ma, 2Applied Phys. Lett., 84 (2004) 4029–4031.

[81] Y.Q. Wang, J.Y. Zhang, X.Q. Liang, K. Wu, G. Liu, J. Sun, Acta Mater., 95 (2015) 132–144.

[82] M. Kapoor, T. Kaub, K.A. Darling, B.L. Boyce, G.B. Thompson, Acta Mater., 126 (2017) 564–575.

[83] R. Lei, M. Wang, S. Xu, H. Wang, G. Chen, Metals

(Basel). 6 (2016) 194.

[84] J.Y. Zhang, J.T. Zhao, X.G. Li, Y.Q. Wang, K. Wu, G. Liu, J. Sun, Acta Mater., 143 (2018) 55–66.

[85] J. Cornejo, V. Martínez, S. Ordoñez, Key Eng. Mater., 189–191 (2001) 561–566.

[86] X. He, X.Y. Li, B.X. Liu, J. Phys. Soc. Japan ,72 (2003) 3032–3034.

[87] S.A. Martynova, E.Y. Filatov, S. V Korenev, N. V Kuratieva, L.A. Sheludyakova, P.E. Plusnin, Y. V Shubin, E.M. Slavinskaya, A.I. Boronin, J. Solid State Chem. 212 (2014) 42–47.

[88] S. Porobova, T. Markova, V. Klopotov, A. Klopotov, O. Loskutov, V. Vlasov, AIP Conf. Proc. 1698 (2016) 2–9.

[89] Y.Z. Tian, Z.F. Zhang, Scr. Mater., 66 (2012) 65–68.

[90] I.H. Lee, S.I. Hong, K.H. Lee, J. Korean Inst. Met. Mater., 50 (2012) 931–937.

[91] K.S. Kormout, B. Yang, R. Pippan, Adv. Eng. Mater., 17 (2015) 1828–1834.

[92] Y.Z. Tian, J.J. Li, P. Zhang, S.D. Wu, Z.F. Zhang, M. Kawasaki, T.G. Langdon, Acta Mater., 60 (2012) 269–281.

[93] Y. Sakai, K. Inoue, H. Maeda, Acta Metall. Mater., 43 (1995) 1517–1522.

[94] Y. Zhong, A. Saengdeejing, L. Kecskes, B. Klotz, Z. Liu, Acta Mater. 61 (2013) 660–669.

[95] D. Liang, Y. Liu, J. Alloys Compd. 426 (2006) 101–105.

[96] G.P. Purja Pun, K.A. Darling, L.J. Kecskes, Y. Mishin, Acta Mater., 100 (2015) 377–391.

[97] K.A. Darling, E.L. Huskins, B.E. Schuster, Q. Wei, L.J. Kecskes, Mater. Sci. Eng. A, 638 (2015) 322–328.

[98] Z. Liu, W. Zhou, Y. Lu, H. Xu, Z. Qin, X. Lu, Mater. Lett., 225 (2018) 85–88.

[99] Q. Zhou, P. Chen, J. Alloys Compd., 657 (2016) 215–223.

[100] C. Jigui, W. Lei, C. Yanbo, Z. Jinchuan, S. Peng, D. Jie, J. Mater. Process. Technol., 210 (2010) 137–142.

[101] J. Li, N. Deng, P. Wu, Z. Zhou, J. Alloys Compd,. 770 (2019) 405–410.

[102] Y. Li, J. Zhang, G. Luo, Q. Shen, L. Zhang, Int. J. Refract. Metals Hard Mater., 71 (2018) 255–261.

[103] H.G. Paris, B.G. LeFevre, Mater. Res. Bull., 7 (1972) 1109–1116.

[104] G.D. Barrera, de R.H. Tendler, E.P. Isoardi, Model. Simul. Mater. Sci. Eng. 8 (2000) 389–401.

[105] A.Y. Volkov, Gold Bull., 37 (2004) 208–215.

[106] A. Rohatgi, K.S. Vecchio, G.T. Gray, Acta Mater., 49 (2001) 427–438.

[107] Y. Zhang, N.R. Tao, K. Lu, Scr. Mater., 60 (2009) 211–213.

[108] P.C.J. Gallagher, Metall. Trans. I, (1970) 2429–2461.

[109] W.Z. Han, Z.F. Zhang, S.D. Wu, S.X. Li, Philos. Mag., 88 (2008) 3011–3029.

[110] T. V Nordstrom, C.R. Barrett, Acta Metall., 17 (1969) 139–146.

[111] W. Ratuszek, A. Bunsh, K. Chrusciel, Mater. Sci. Forum, 157–162 (1994) 1045–1050.

[112] S.N. Dey, P. Chatterjee, S.P. Sen Gupta, J. Appl. Phys., 100 (2006) 073509.

[113] X.L. Ma, W.Z. Xu, H. Zhou, J.A. Moering, J. Narayan, Y.T. Zhu, Philos. Mag., 95 (2015) 301–310.

[114] Y.H. Zhao, X.Z. Liao, Y.T. Zhu, Z. Horita, T.G. Langdon, Mater. Sci. Eng. A 410–411 (2005) 188–193.

[115] S.K. Chatterjee, S.K. Halder, S.P. Sen Gupta, J. Appl. Phys., 48 (1977) 1442–1448.

[116] S. Fujita, T. Uesugi, Y. Takigawa, K. Higashi, Mater. Sci. Forum, 561–565 (2007) 1915–1918.

[117] H.P. Rave, E. Hombogen, Z. Met., 55 (1964) 763.

[118] A. Vinogradov, D.L. Merson, V. Patlan, S. Hashimoto, Mater. Sci. Eng. A, 341 (2003) 57–73.

[119] S.K. Ghosh, S.P. Sen Gupta, J. Appl. Phys., 54 (1983) 6652.

[120] S.N. Dey, P. Chatterjee, S.P. Sen Gupta, Acta Mater., 53 (2005) 4635–4642.

[121] N.M. Heckman, L. Velasco, A.M. Hodge, MRS Commun., 1 (2017) 6–11.

[122] Y.Z. Tian, L.J. Zhao, S. Chen, A. Shibata, Z.F. Zhang, N. Tsuji, Nat. Sci. Reports, 5 (2015) 16707.

[123] L. Velasco, M.N. Polyakov, A.M. Hodge, Scr. Mater., 83 (2014) 33–36.

[124] M. Makhlouf, T. Bachaga, J. Sunol, M. Dammak, M. Khitouni, Metals (Basel)., 6 (2016) 145.

[125] X.H. An, S.D. Wu, Z.F. Zhang, R.B. Figueiredo, N. Gao, T.G. Langdon, Scr. Mater. 66 (2012) 227–230.

[126] C.X. Huang, W. Hu, G. Yang, Z.F. Zhang, S.D. Wu, Q.Y. Wang, G. Gottstein, Mater. Sci. Eng. A,556 (2012) 638–647.

[127] C.S. Barrett, J. Met., 188 (1950) 123–135.

[128] B.G. Mendis, I.P. Jones, R.E. Smallman, J. Electron Microsc. (Tokyo)., 53 (2004) 311–323.

[129] H. Saka, Philos. Mag. A, 47 (1983) 131–140.

[130] K. Sufryd, N. Ponweiser, P. Riani, K.W. Richter, G. Cacciamani, Intermetallics, 19 (2011) 1479–1488.

[131] R.H. Jo, T.J. Kim, S.H. Hong, Y.S. Kim, H.J. Park, W.J. Park, J.M. Park, B.K. Kim, J. Alloys Compd., 707 (2017) 184–188.

[132] G.H. Xiao, N.R. Tao, K. Lu, Scr. Mater., 59 (2008) 975–978.

[133] K. Youssef, M. Sakaliyska, H. Bahmanpour, R. Scattergood, C. Koch, Acta Mater., 59 (2011) 5758–5764.

[134] K.H.G. Ashbee, L.F. Vassamillet, Acta Metall., 15 (1967) 481–484.

[135] Y.L. Gong, C.E. Wen, Y.C. Li, X.X. Wu, L.P. Cheng, X.C. Han, X.K. Zhu, Mater. Sci. Eng. A, 569 (2013) 144–149.

[136] L. Delehouzee, A. Deruyttere, Acta Metall., 15 (1967) 727–734.

[137] R. Juškenas, Z. Mockus, S. Kanapeckaite, G. Stalnionis, A. Survila, Electrochim. Acta, 52 (2006) 928–935.

[138] X. Sang, K. Du, H. Ye, J. Alloys Compd., 469 (2009) 129–136.

[139] Y. Zhang, D.W. Yuan, J.H. Chen, G. Zeng, T.W. Fan, Z.R. Liu, C.L. Wu, L.H. Liu, J. Electron. Mater., 45 (2016) 4018–4027.

[140] Y. Cao, S. Ni, X. Liao, M. Song, Y. Zhu, Mater. Sci. Eng. R, 133 (2018) 1–59.

GENERALIZOVANE ENERGIJE GREŠAKA PAKOVANJA LEGURA BAKRA – IZRAČUNAVANJE PO TEORIJI FUNKCIONALA GUSTINE

M. Muzyk [a*] and K.J. Kurzydlowski [b]

[a*] Fakultet za matematiku i prirodne nauke, Odsek za egzaktne nauke, Univerzitet kardinala Stefana Vižinjskog u Varšavi, Varšava, Poljska
[b] Mašinski fakultet, Tehnološki univerzitet u Bialistoku, Białistok, Poljska

Apstrakt

Generalizovane energije grešaka pakovanja legura bakra izračunate su pomoću teorije funkcionala gustine. Energija grešaka pakovanja je u korelaciji sa brojem d elektrona prelaznog metala legirajućeg elementa u ravni deformacije. Tendencija ka dvojnikovanju je takođe modifikovana prisustvom legirajućeg elementa u ravni deformacije. Rezultati ukazuju da se od Cu –legura prelaznog metala sa elementima kao što su Cr, Mo, W i Mn očekuje da pokažu izuzetnu brzinu očvršćavanja zbog tendencije ka emisiji parcijalnih dislokacija.

Ključne reči: Ab initio izračunavanja; Legure bakra; Dvojnikovanje